Polymorphic population expansion velocity in a heterogeneous environment

Lionel Roques, Nathanaël Boutillon, Patrizia Zamberletti, Julien Papaïx

Polymorphic population expansion velocity in a heterogeneous environment

L. Roques[a,*], N. Boutillon[a,b], P. Zamberletti[a], J. Papaïx[a]

[a] INRAE, BioSP, 84914, Avignon, France

[b] Aix Marseille Univ, CNRS, I2M, Marseille, France

[*] Corresponding author: lionel.roques@inrae.fr

Abstract

How does the spatial heterogeneity of landscapes interact with the adaptive evolution of populations to influence their spreading speed? This question arises in agricultural contexts where a pathogen population spreads in a landscape composed of several types of crops, as well as in epidemiological settings where a virus spreads among individuals with distinct immune profiles. To address it, we introduce an analytical method based on reaction-diffusion models. We focus on spatially periodic environments with two distinct patches, where the dispersing population consists of two specialized morphs, each potentially mutating to the other. We present new formulas for the speed together with criteria for persistence, accounting for both rapidly and slowly varying environments, as well as small and large mutation rates. Altogether, our analytical and numerical results yield a comprehensive understanding of persistence and spreading dynamics. In particular, compared to a situation without mutations or to a single morph spreading in a heterogeneous landscape, the introduction of mutations to a second morph with reverse specialization, while consistently impeding persistence, can significantly increase speed, even if the mutation rate between the two morphs is very small. Additionally, we find that the amplitude of the spatial fragmentation effect is significantly increased in this case. This has implications for agroecology, emphasizing the higher importance of landscape structure in influencing adaptation-driven population dynamics.

Keywords: expansion speed; adaptation; mutation; heterogeneity; reaction-diffusion

1 Introduction

One of the major aspects that has contributed to the success of reaction-diffusion approaches in spatial ecology is that their results can sometimes be expressed in the

form of simple mathematical expressions. The most famous example is the Fisher-KPP model in a homogeneous one-dimensional environment. In the context of this model, a population that is initially confined to a limited area will spread with a speed $c = 2\sqrt{r\,D}$. This very simple formula provides valuable insight into the effects of the intrinsic growth rate (r) and the spatial diffusion parameter (D) on the speed at which the population spreads. This formula has had a considerable impact on theoretical ecology (e.g. Skellam, 1951; Mollison, 1991; Okubo and Levin, 2002), whether in describing biological invasions or epidemiological phenomena. One can wonder if obtaining so simple formulas remains feasible as the model becomes more realistic.

The study of local adaptation and its role in driving population dynamics in heterogeneous environments has received considerable attention, both from an experimental and a theoretical perspective, see Kawecki and Ebert (2004) and references therein. Local adaptation is a process whereby subpopulations evolve, through Darwinian selection, to become better adapted to their local environment (Williams, 2018). In the absence of forces beyond Darwinian selection, genotype-environment interactions should cause each local population to adapt to its specific environmental conditions, regardless of the conditions present in other regions of space. We consider here the case of an asexual population expanding its spatial range in a heterogeneous environment. Then, several factors can prevent the population from reaching the local adaptive optimum, and can influence the spreading speed of the population. These factors include the mutation load (i.e. the reduction in the average fitness of a population due to the accumulation of deleterious mutations Kimura and Maruyama, 1966; Martin and Gandon, 2010), and migration of individuals from other regions of space (Débarre et al., 2013); see also (Pease et al., 1989; Kirkpatrick and Barton, 1997) for similar effects in sexually-reproducing populations. In addition to these evolutionary effects, the amplitude and spatial distribution of heterogeneities also contribute to the overall picture, as they are known to impact the spreading speed in non-adaptive contexts (Shigesada and Kawasaki, 1997; Berestycki et al., 2005b); see also (Cruywagen et al., 1996) in the case of two competing species. In this work, we propose a method to characterize analytically, in some limiting cases, the spreading speed in models involving both spatial heterogeneity of the environment and adaptive evolution of the population.

The motivation for this work stems from the shift from an intensive cropping system supported by uniform agricultural landscapes to the agroecology paradigm, where crop diversification plays a central role to ensure the stability of yields (Gascuel-Odoux et al., 2022; Caquet et al., 2020; Food and Agriculture Organization of the United Nations, 2018; Beillouin et al., 2021). In particular, host diversity is known to influence disease spread through various mechanisms (Keesing et al., 2006), one of which results from the interplay between the dispersal and competition among pathogen genotypes that adapt differentially to the various hosts present in the environment (Borg et al., 2018). In this context, most studies emphasize the role of host diversity in shaping pathogen evolution (Débarre and Gandon, 2010), pathogen diversity (Papaix et al., 2014), and the risk of disease persistence (Lively, 2010). However, it is interesting to note that little effort has been dedicated to understanding how host diversity affects the speed of

disease spread.

In heterogeneous spatially-periodic environments, and with a unique morph (i.e., without adaptation), Fisher-KPP type models have also seen some success, yielding numerous results on the connections between the spatial structure of the environment, persistence, and spreading (Shigesada and Kawasaki, 1997; Weinberger, 2002; Berestycki et al., 2005a,b). However, these connections have generally only been described in a qualitative manner, through results such as monotonic dependence between parameters characterizing the environment and quantities characterizing persistence and spreading. In particular, "Freidlin-Gärtner" formulas for the spreading speed are not as explicit as the formula $c = 2\sqrt{r\,D}$ when $r(x)$ and $D(x)$ depend on the space variable x. One way to overcome this issue is to look at the limiting cases of small and large periods L, which respectively correspond to highly-fragmented and low-fragmented environments. The case of small periods naturally leads to a homogenization limit and a simple formula $c(L \to 0) = 2\sqrt{\langle r\rangle_a \langle D\rangle_h}$, where $\langle r\rangle_a$ is the arithmetic mean of $r(x)$ and $\langle D\rangle_h$ is the harmonic mean of $D(x)$ over a period cell. This formula was originally derived by Shigesada et al. (1986) for coefficients that vary sinusoidally and extended to general diffusion and growth rate profiles in (El Smaily et al., 2009). It can be complemented by studying the other limit, where the period length becomes very large, to better capture the effect of heterogeneities (Hamel et al., 2010, 2011).

When adaptation occurs, the expanding population may consist of multiple morphs, each specializing in a limited number of hosts. In this scenario, polymorphism in life history traits among individuals, as discussed by (Elliott and Cornell, 2012) and (Morris et al., 2019), has the potential to influence the invasion speed. Both studies primarily focus on dispersal polymorphism and the complementarity between strategies that invest in growth and those that invest in dispersal. However, they considered only homogeneous environments. Our goal in this study is to examine the influence of adaptation on the spreading speed of a species within a heterogeneous environment. We specifically analyze scenarios in which the environment is periodic, consisting of two distinct patches. The spreading population is made up of two unique morphs, each specialized for one of the patch types. Crucially, part of the offspring of one morph can mutate at birth to become the other morph. We anticipate that the interaction between the two morphs will have a significant impact on the spreading speed. Some parameters can exhibit dual effects. For instance, a higher mutation rate is known to increase the mutation load and decrease the time needed for local environment adaptation (Anciaux et al., 2019; Lavigne et al., 2020). Predicting the effect of the mutation rate on the spreading speed, therefore, becomes a complex endeavor. Explicit analytic formulas will offer valuable insight into the intertwined roles of adaptive, demographic, and spatial factors.

Recent formulas have been derived (Griette and Matano, 2021), but they tend to be abstract and provide limited ecological insight. In this study, we present new formulas for the speed, accounting for both rapidly and slowly varying environments, as well as for small and large mutation rates. The rapidly varying environment limit is a direct consequence of the results in Griette and Matano (2021). In contrast, deter-

mining the speed for slowly varying environments is notably more intricate and unveils some unexpected results, which stand as the cornerstone of our research. Altogether, our formulas, complemented by insight from numerical simulations, enhance our understanding of the specific impacts, on the expansion of the population, of the mutation rate and of the environmental fragmentation. In particular, our research reveals that allowing mutations between the two morphs results in a sudden increase of the speed, with respect to the scenario without mutations; this emerges as one of the primary and significant results of the paper.

2 Material and methods

2.1 Model development

The model describes the spread of two distinct morphs of a single species within a heterogeneous 1-dimensional environment composed of two types of patches. This scenario mimics the spreading of pathogens in an environment with alternating hosts, see Figure 1 for a schematic description of the model. The two morphs are differentiated by their varying fitness levels (i.e. their growth rates), and interact through local competition. Additionally, a portion of the offspring of one morph may switch to the other morph through the process of mutation at birth (we assume here that the growth terms depend on the morph and on x only through the death rate; the birth rate is independent of x). The spread of these morphs is further influenced by spatial diffusion. We represent the overall dynamics of this system with the following reaction-diffusion model:

$$\begin{cases} \partial_t u(t,x) = & D\,\partial_{xx} u + r_L^u(x)\,u - \gamma_L(x)\,u\,(u+v) + \mu\,(v-u), \\ \partial_t v(t,x) = & D\,\partial_{xx} v + r_L^v(x)\,v - \gamma_L(x)\,v\,(u+v) + \mu\,(u-v), \end{cases} \quad t>0,\ x\in\mathbb{R}. \tag{1}$$

In this context, x represents the spatial variable, while $u(t,x)$ and $v(t,x)$ are the population densities of the two morphs. The periodic functions $r_L^u(x)$ and $r_L^v(x)$ are the growth rates of the two morphs (which depend on the spatial position x). Additionally, D is the spatial diffusion coefficient, which is constant in space and shared by both morphs, and μ is a coefficient proportional to the mutation rate. Finally, $\gamma_L(x)$ is a competition coefficient. The environment, described by the functions r_L^u and r_L^v, is assumed to be periodic with a period L, where one half $[0, L/2)$ of the period cell corresponds to the first host, and the other half $[L/2, L)$ corresponds to the second host. Namely,

$$r_L^u(x) = r^u(x/L),\ r_L^v(x) = r^v(x/L) \text{ and } \gamma_L(x) = \gamma(x/L), \tag{2}$$

where r^u, r^v and γ are 1-periodic functions. We assume that the two morphs have distinct specializations. One morph has a higher growth rate ($R^+ > 0$) on one of the patches and a lower growth rate ($R^- \le R^+$) on the other patch, while the other morph has the opposite specialization. In other words

$$\begin{cases} r_L^u(x) = R^+ \text{ and } r_L^v(x) = R^- \text{ for } x\in[0,L/2), \\ r_L^u(x) = R^- \text{ and } r_L^v(x) = R^+ \text{ for } x\in[L/2,L). \end{cases} \tag{3}$$

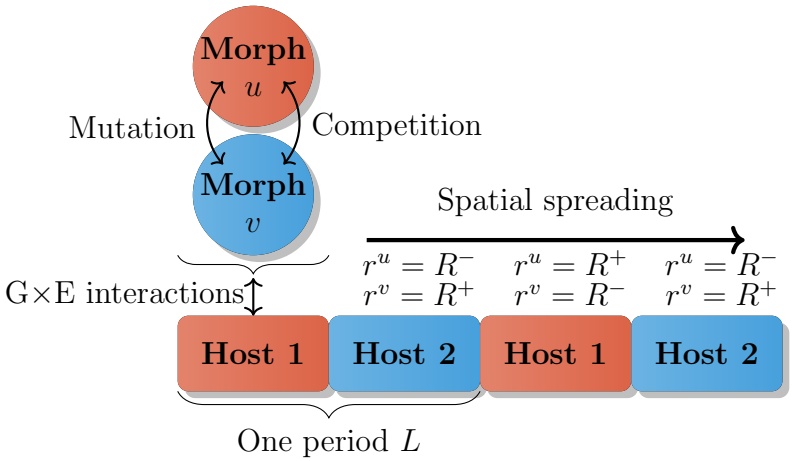

Figure 1: Schematic representation of the model in a spatially periodic environment. Morphs u and v have specialized interactions with their hosts: morph u has fitness R^+ on host 1 and R^- on host 2, and conversely morph v has fitness R^- on host 1 and R^+ on host 2 ($R^+ > R^-$). The horizontal arrow signifies spatial spreading of the morphs through the environment.

Persistence of the population. As shown in Theorem 2.9 of Griette and Matano (2021), the persistence or extinction of the population $u+v$ depends on the sign of $k_0^{2\,m}$, the principal eigenvalue of an elliptic operator $\mathcal{L}_0^{2\,m}$, that indicates whether the state $(u, v) = (0, 0)$ is stable or not (see Appendix A). Here, "$2\,m$" stands for 2 morphs; in contrast, $k_0^{1\,m}$ corresponds to the 1 morph case.

When we study the spreading properties, we always assume that $k_0^{2\,m} > 0$, which ensures the persistence of the population. In our framework, a simple sufficient condition for this is $R^+ + R^- > 0$ (see Appendix A). We obtain exact persistence conditions through explicit relations between R^+, R^-, μ and $k_0^{2\,m}$ in the four limiting cases $L \to 0$, $L \to \infty$, $\mu \to 0$ and $\mu \to \infty$. We will describe them in Section 3.

Spreading properties. In the case of a spatially homogeneous environment, i.e., when the coefficients do not depend on x, Girardin (2017) established the spreading properties of the system (1). The recent results of Griette and Matano (2021) extend these properties to systems with spatially periodic coefficients. Before going further on, we need to introduce precisely the notion of spreading speed. The spreading speed to the right (the spreading speed to the left could be considered as well) is the asymptotic rate at which a species, initially concentrated in a bounded spatial region, expands its spatial range to the right-hand side of the 1-dimensional environment (Aronson and Weinberger, 1975). See also Weinberger (2002) for a definition in a spatially-periodic setting. In our setting, with two morphs and with a spatially-periodic heterogeneity, the spreading speed can be defined in the following way. If an observer travels to the right (i.e., towards increasing x values) above that speed, the observer will see the

total population density $u(t,x)+v(t,x)$ vanish. If the observer travels to the right below that speed, the observer will not see the total population density vanish. In mathematical terms, we consider initial conditions (u_0, v_0) which are nonnegative, not identically equal to $(0,0)$ and such that $(u_0(x), v_0(x)) = 0$ for all x large enough. Then, $c^{2\,m}$ is the spreading speed associated with the system (1) if

$$\begin{aligned} \lim_{t\to\infty} \sup_{x\geq w'\,t} u(t,x)+v(t,x) = 0 \quad &\text{for all } w' > c^{2\,m}, \\ \liminf_{t\to\infty} \inf_{x\leq w''\,t} u(t,x)+v(t,x) \neq 0 \quad &\text{for all } w'' < c^{2\,m}. \end{aligned} \tag{4}$$

Let us first focus on the particular case $\mu = 0$: There are no mutations between the two morphs. Since the speed depends on the linearization of the system at $(0,0)$ (Griette and Matano, 2021), the competition between the two morphs has no influence on the spreading speed. With this assumption, the spreading speed is the same as with a single morph ($c^{2\,m} = c^{1\,m}$), say u, in a heterogeneous environment: $\partial_t u(t,x) = d\,\partial_{xx} u + r_L^u(x)\,u - \gamma_L(x)\,u^2$. In this case, the existence of a spreading speed is well-known, as well as its dependence with respect to the period L, as we mentioned in the Introduction. In particular, the limit of rapidly oscillating environments (small values of L) has been studied extensively (Shigesada et al., 1986; El Smaily et al., 2009; Kinezaki et al., 2006): the spreading speed converges to the speed in a spatially averaged medium, where the growth rate is replaced by its mean value $(R^+ + R^-)/2$. Namely, $c^{1\,m}(L\to 0) = \sqrt{2\,D\,(R^+ + R^-)}$. The other limit, of slowly oscillating environments, was studied in Hamel et al. (2010). Their results imply that

$$c^{1\,m}(L\to\infty) = 4\sqrt{D} \times \frac{(R^+)^2 + (R^-)^2 + (R^+ + R^-)\sqrt{\triangle}}{(R^+ + R^- + 2\sqrt{\triangle})^{\frac{3}{2}}}, \tag{5}$$

with $\triangle = (R^+)^2 + (R^-)^2 - R^+R^-$. In cases where $R^- = 0$, the expression simplifies to

$$c^{1\,m}(L\to\infty) = (8/9)\sqrt{3\,D\,R^+} \simeq 1.53\sqrt{DR^+}.$$

Hamel et al. (2011) also considered more general forms for the reaction and diffusion coefficients. The dependence of the spreading speed on the parameter L has also been recently analyzed: the velocity has been found to be an increasing function of the period L, first numerically for some specific examples in Shigesada and Kawasaki (1997); Kinezaki et al. (2003), then analytically for the general case in Nadin (2010). This set of results provided a better understanding of the effect of resource fragmentation on the rate of spread of a single-morph population, in the absence of adaptation. In particular, because of the monotonicity of the spreading speed with respect to L, the difference $c^{1\,m}(L\to\infty) - c^{1\,m}(L\to 0)$ provides a quantitative measure of the potential effect of fragmentation.

Our objective in this study is to explore the scenario where $\mu > 0$. The existence of a spreading speed follows from Griette and Matano (2021) (under the condition for persistence $k_0^{2\,m} > 0$). The results in Griette and Matano (2021) imply that this

spreading speed is characterized by the following formula:

$$c^{2\,m} = \min_{\lambda>0} \frac{k_\lambda}{\lambda}, \tag{6}$$

where k_λ is the unique real number (principal eigenvalue) such that there exists a pair of positive L-periodic functions (ϕ_1, ϕ_2) satisfying:

$$\begin{cases} D\,\phi_1'' + 2\,\lambda\,D\,\phi_1' + \lambda^2\,D\,\phi_1 + r_L^u(x)\,\phi_1 + \mu(\phi_2 - \phi_1) &= k_\lambda\,\phi_1, \\ D\,\phi_2'' + 2\,\lambda\,D\,\phi_2' + \lambda^2\,D\,\phi_2 + r_L^v(x)\,\phi_2 + \mu(\phi_1 - \phi_2) &= k_\lambda\,\phi_2, \end{cases} \text{ in } \mathbb{R}. \tag{7}$$

This type of "Freidlin-Gärtner" formula is classical in the scalar case (i.e., with one morph Freidlin and Gärtner, 1979; Weinberger, 2002; Berestycki et al., 2008). For systems such as (1), such a formula was first proved by Girardin (2017) when the coefficients do not depend on x, and then extended by Griette and Matano (2021) to the general case. This theoretical formula, however, provides limited ecological insight. In this work, we derive explicit formulas for $c^{2\,m}$, in the limit of rapidly varying ($L \to 0$) and slowly varying environments ($L \to \infty$) and in the limit of small mutations ($\mu \to 0$) and large mutations ($\mu \to \infty$).

Numerical computations. We present a novel algorithm designed to numerically compute the speed $c^{2\,m}$. Our approach involves a finite difference approximation of the operator in (7), accounting for periodic conditions. Subsequently, we employ standard matrix methods (SciPy and ARPACK libraries using the eigs function) to determine the principal eigenvalue k_λ for discrete λ values. This information is then used in conjunction with the formula (6) to yield an approximate computation $c_{sim}^{2\,m}$ of $c^{2\,m}$. A Jupyter notebook is available at `https://doi.org/10.17605/OSF.IO/7RTFK`. It can be easily launched on Google Colab, requiring no technical skills. We also developed a basic finite difference algorithm to visualize the solutions of the system (1). It is used here for illustrative purposes and is notably less accurate when compared to the other code used for speed computation. This code is also available as Jupyter notebook (same url).

3 Main results

Persistence. We are equipped to provide a quantitative criterion for persistence in the limit of small or large periods and mutation rates. The outcomes are succinctly summarized in Table 1 and substantiated in Appendix A. Most of these results are intuitive and are direct consequences of the Rayleigh formula, see (A.3)-(A.4) in Appendix A.

In the scenario of rapidly varying environments ($L \to 0$), the application of homogenization techniques allows the replacement of r_L^u and r_L^v by their spatial mean value $(R^+ + R^-)/2$, resulting in the convergence of $k_0^{2\,m}$ to $(R^+ + R^-)/2$. As the period L increases, $k_0^{2\,m}$ also increases and converges as $L \to +\infty$ towards

$$\frac{1}{2}\sqrt{(R^+ - R^-)^2 + 4\,\mu^2} - \mu + (R^+ + R^-)/2,$$

μ \ L	$L \to 0$	Arbitrary L	$L \to \infty$
$\mu = 0$	$R^+ + R^- > 0$	$k_0^{1\,m} > 0$	$R^+ > 0$
$\mu \to 0$	$R^+ + R^- > 0$	$k_0^{1\,m} > 0$	$R^+ > 0$
Arbitrary μ	$R^+ + R^- > 0$	$k_0^{2\,m} > 0$	$R^+ > \frac{\mu}{1+(\mu/(-R^-))}$ or $R^+ + R^- > 0$
$\mu \to \infty$	$R^+ + R^- > 0$	$R^+ + R^- > 0$	$R^+ + R^- > 0$

Table 1: Criterion for persistence. The result remains unchanged whether the limit is taken first in μ or L. Respectively, $k_0^{1\,m}$ and $k_0^{2\,m}$ correspond to the principal eigenvalues that determine the persistence condition for a one-morph problem and a two-morph problem, see formulas in Appendix A. The condition $R^+ > \mu/(1 + (\mu/(-R^-))$ is valid when $R^- < 0$; otherwise persistence always holds for $R^+ > R^- > 0$.

which leads to the condition $R^+ > \mu/[1 + (\mu/(-R^-))]$ for persistence. The limit value of $k_0^{2\,m}$ as $L \to +\infty$ is the principal eigenvalue for a homogeneous environment where $r_L^u = R^+$ and $r_L^v = R^-$: in the case of very large periods, the influence of spatial variations on persistence becomes negligible. We can observe from formulas (A.3)-(A.4) in Appendix A, that $k_0^{2\,m}$ increases with L and decreases with D. Additionally, $k_0^{2\,m}$ decreases as μ increases. This implies that the impact of the mutation load outweighs other plausible beneficial effects of mutation. Consequently, as far as the population persistence is concerned, the potential to mutate into an alternative morph with a distinct adaptive profile consistently proves unfavorable (i.e., $k_0^{2\,m} < k_0^{1\,m}$ when $\mu > 0$). It is worth noting that the instances of $\mu = 0$ and $\mu \to 0$ are the same; the criterion characterizing the persistence behavior is continous at $\mu = 0$, even when $L \to \infty$.

We notice that under our assumptions, where the growth rates r^u and r^v of the two morphs are symmetric (i.e. they mirror each other), the order of the limits taken with respect to μ and L can be interchanged in Table 1 without altering the outcomes. Moreover, the limits as $L \to 0$ and as $\mu \to \infty$ lead to the same homogenization result. This actually conceals differences in the effects of these two limit transitions, which are elucidated in the proofs presented in Appendix A. The case of $L \to 0$ corresponds to spatial homogenization (where r^u and r^v are replaced by their respective spatial averages), whereas the case of $\mu \to \infty$ corresponds to homogenization between the two morphs, but in a local spatial context (where $r^u(x)$ and $r^v(x)$ are replaced at each spatial point x by their average value $(r^u(x) + r^v(x))/2$). Without the symmetry assumption on r^u and r^v, there is no reason to expect that the limit $L \to 0$ should give the same behavior as the limit $\mu \to \infty$.

Spreading speed. We obtain an analytical charaterization of the spreading speed in rapidly ($L \to 0$) and slowly ($L \to \infty$) varying environments, see Table 2 and Appendix B for technical details. In particular, we prove that, for arbitrary μ,

$$c^{2\,m}(L \to 0) = \sqrt{2D(R^+ + R^-)}, \tag{8}$$

μ \ L	$L \to 0$	Arbitrary L	$L \to \infty$
$\mu = 0$	$\sqrt{2D(R^+ + R^-)}$	$c^{1\,m}$	$c^{1\,m}(L \to \infty)$, see (5)
$\mu \to 0$	$\sqrt{2D(R^+ + R^-)}$	$c^{1\,m}$	$\mu \to 0$ then $L \to \infty$: $c^{1\,m}(L \to \infty)$, see (5) $L \to \infty$ then $\mu \to 0$: $2\sqrt{D\,R^+}$
Arbitrary μ	$\sqrt{2D(R^+ + R^-)}$	Fig. 3	$\sqrt{2D\left(R^+ + R^- + \sqrt{(R^+ - R^-)^2 + 4\,\mu^2} - 2\mu\right)}$
$\mu \to \infty$	$\sqrt{2D(R^+ + R^-)}$	$\sqrt{2D(R^+ + R^-)}$	$\sqrt{2D(R^+ + R^-)}$

Table 2: Spreading speed $c^{2\,m}$. Except for the limit $(L, \mu) \to (+\infty, 0)$, the results remain unchanged whether the limit is taken first in μ or L. The notation $c^{1\,m}$ stands for the spreading speed when there is only one morph.

and that

$$c^{2\,m}(L \to \infty) = \sqrt{2D\left(R^+ + R^- + \sqrt{(R^+ - R^-)^2 + 4\,\mu^2} - 2\mu\right)}. \tag{9}$$

Interestingly, although the model with two morphs is more intricate, the limiting spreading speed as $L \to +\infty$ is given by a formula (9) which seems simpler than the corresponding formula for the one morph model, see (5). In the limit $L \to \infty$, we observe that $c^{2\,m}$ is a decreasing function of the mutation coefficient: the highest speeds are achieved when $\mu \to 0$. In the limit $\mu \to 0$, $c^{2\,m} \to 2\sqrt{D\,R^+}$, which corresponds to the spreading speed of a single morph in a homogeneous and favourable environment (i.e., with constant growth rate R^+). Interestingly, this speed is much larger than in the case $\mu = 0$, see (5). This is more obvious in the case $R^- = 0$: when $\mu = 0$ we have $c^{2\,m}(L \to \infty) = c^{1\,m}(L \to \infty) = (8/9)\sqrt{3\,D\,R^+} \approx 1.54\,\sqrt{D\,R^+}$, to be compared to the limit $2\sqrt{D\,R^+}$ of $c^{2\,m}(L \to \infty)$ as $\mu \to 0$, which is 30% larger. Thus, the function $\mu \mapsto c^{2\,m}(L \to \infty)(\mu)$ admits a discontinuity at $\mu = 0$. Figure 2a illustrates solutions of the system (1), both with $\mu > 0$ and with $\mu = 0$, starting from the same compactly supported initial condition. The figure shows that the spreading is indeed faster when $\mu > 0$. This is corroborated in Figure 2b, which tracks the position of a level of $u + v$ over time. In particular, in the case of $\mu > 0$, the instantaneous speed is much less variable than in the case of $\mu = 0$.

Figure 3 gives a numerical description of the relationship between the speed c^{2m} and the parameters μ and L. It shows that, even if this discontinuity does not appear for finite values of L, there is a significant jump in speed for small values of μ. This sudden jump is particularly pronounced as L increases, demonstrating that the presence of a second morph may hold a more significant influence under such circumstances for large periods. The speed culminates at an optimum mutation rate, and after the optimal μ value, the speed becomes a decreasing function of μ, highlighting the dominance of the emergence of ill-adapted mutants (mutation load). According to Figure 3, the

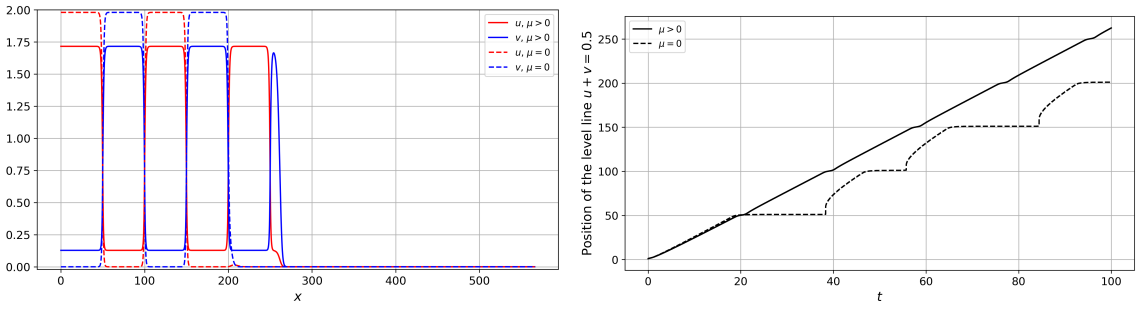

(a) (b)

Figure 2: **Solutions of the main system** (1)**,** $\mu > 0$ **vs** $\mu = 0$**.** (a) The solutions are plotted at time $t = 100$; (b) Dynamics of the position of 0.5 level line of $u + v$, defined as the rightmost point $x_{0.5}(t)$ where $(u + v)(t, x_{0.5}(t)) = 0.5$. The parameter values are $R^+ = 2$, $R^- = 0$, $D = 1$, $\mu = 0.15$, $L = 100$ and the initial condition $u(0, x) = v(0, x) = 1$ for $x \leq 1$ and $u(0, x) = v(0, x) = 0$ for $x > 1$.

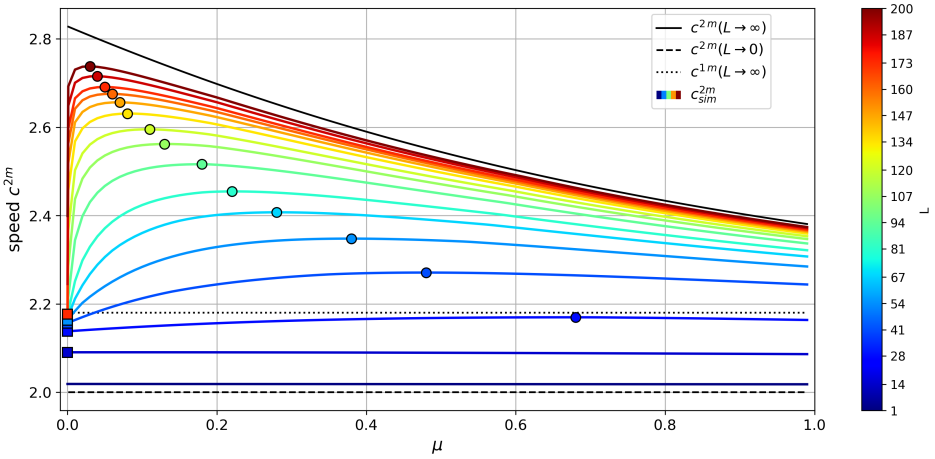

Figure 3: **Theoretical and simulated speeds in terms of the mutation parameter** μ **and spatial period** L**.** The circles indicate the maximum values of $c^{2\,m}_{sim}$, for each L. The leftmost points ($\mu = 0$, squares) indicate the numerical value of the speed $c^{1\,m}_{sim}$. The parameter values are $R^+ = 2$, $R^- = 0$, $D = 1$, leading to $c^{1\,m}(L \to 0) = 2$, $c^{2\,m}(L \to 0) = 2$, $c^{1\,m}(L \to \infty) \approx 2.18$, $c^{2\,m}(L \to \infty) = 2\sqrt{2} \approx 2.83$ as $\mu \to 0$, see Table 2.

optimal value for the mutation rate μ decreases as L is increased, indicating that this mutation load effect arises sooner in low-fragmented environments. Consistently with our knowledge in the case of a single morph (Shigesada and Kawasaki, 1997; Kinezaki et al., 2003; Nadin, 2010), we also observe in Figure 3 that the spreading speed increases with the period L, beginning at $c^{2\,m}(L \to 0)$ and reaching its maximum at $c^{2\,m}(L \to \infty)$. However, we observe that the range of variation, as indicated by the difference between the dashed and solid lines in Figure 3, is much more important in this context compared to the case of a single morph, where the difference is between the dashed and dotted lines in Figure 3. This also follows from the results in Table 2. For instance, in the particular case $R^- = 0$ (as in Figure 3), the table shows that the maximum amplitude of variation as L is increased is $c^{1\,m}(L \to \infty) - c^{1\,m}(L \to 0) = ((8/9)\sqrt{3} - \sqrt{2})\sqrt{D\,R^+} \approx 0.13\sqrt{D\,R^+}$ in the case of one morph, vs $c^{2\,m}(L \to \infty) - c^{2\,m}(L \to 0) = (2 - \sqrt{2})\sqrt{D\,R^+} \approx 0.59\sqrt{D\,R^+}$ in the case of two morphs, for small μ.

When μ tends towards infinity, the spreading speed $c^{2\,m}(\mu \to \infty)$ converges to $\sqrt{2\,D\,(R^+ + R^-)}$, signifying yet another homogenization limit. The system operates as though there were a single morph with a uniform growth rate of $(R^+ + R^-)/2$. Similar to our earlier observations on persistence, this homogenization remains spatially local in the sense that large mutation rate induces the replacement of the growth rates r^u and r^v at each spatial point x by their averaged value $(r^u(x) + r^v(x))/2$.

Let us now state a conjecture for a general formula describing the limit spreading speed as L approaches infinity, considering arbitrary 1-periodic functions r^u and r^v. This means that we no longer assume these functions to be piecewise constant or to mirror each other. The idea is to adapt the results presented in Hamel et al. (2011), which addressed the limit as L tends to infinity for the critical invasion speed $c^{1\,m}$ in scenarios involving only one morph. This concept is elaborated upon in Appendix C, where we aim at establishing a formula applicable when both r^u and r^v are spatially constant and then extend it to accommodate scenarios where these functions are not necessarily constant. Our argument is based on the observation that as the period becomes large, an individual should die before it manages to reach locations where the values of r^u and r^v deviate significantly from their values at the place of birth of the individual. Consequently, throughout its lifespan, an individual encounters nearly constant values of r^u and r^v. This leads us to propose the following conjecture.

Assume that r^u and r^v are arbitrary 1-periodic functions, and that persistence occurs (e.g., $\int_0^1 r^u + r^v > 0$). Define

$$j(k) := \int_0^1 \sqrt{k - \frac{1}{2}\left[r^u(x) + r^v(x) - 2\mu + \sqrt{(r^u(x) - r^v(x))^2 + 4\mu^2}\right]}\,dx.$$

Then j is defined on a maximal interval of definition $[M, +\infty)$ (for some $M > 0$) and

$$c^{2\,m}(L \to \infty) = \sqrt{D} \inf_{\lambda \geq j(M)} \frac{j^{-1}(\lambda)}{\lambda}. \tag{10}$$

For instance, consider the scenario where r^u and r^v alternately take two values, denoted again as R^+ and R^-, such that $r^u(x) = R^+$ if and only if $r^v(x) = R^-$. In this case, we obtain formula (9). It is important to note that this result does not depend on the positions and sizes of the patches where $r^u = R^+$ in relation to those where $r^u = R^-$. This suggests that formula (9) should remain valid under more general assumptions than our initial ones.

Although the formula in (10) seems quite complex, it allows us to establish that $c^{2\,m}(L \to \infty)$ should be a decreasing (or nonincreasing) function of μ in the general case. Furthermore, it enables us to explore other biological scenarios, such as variations in diffusion terms, as discussed in Elliott and Cornell (2012); Morris et al. (2019) in the spatially homogeneous case, or the comparison between generalist and specialist strategies, as detailed in Appendix C.

4 Discussion

In this study, by using the period length as a proxy for the fragmentation of the environment, and by considering a simplified scenario involving a population made up of two morphs, we examined the intertwined influences of habitat heterogeneity, fragmentation, and adaptation. Our analytical and numerical results clarify how these various factors affect the persistence and spreading of the population. In particular, the introduction of mutations always leads to a decreased ability of persistence with respect to the setting without mutations. In some sense, mutation acts as a dispersal term along a phenotypic dimension. Similar to spatial diffusion in classical periodic Fisher-KPP models (Shigesada and Kawasaki, 1997; Berestycki et al., 2005a), mutations reduce persistence by displacing individuals away from the optimal phenotype. Conversely, the introduction of mutations may lead to an increased spreading speed. This means that invasion dynamics can be "anomalous," i.e., faster than any of the morphs in isolation (Weinberger et al., 2007). Since the work of Weinberger et al. (2007), several studies have focused on this type of phenomenon in spatially homogeneous landscapes, see Holzer (2014) in a system of two Fisher-KPP equations with unidirectional coupling, and Poloni and Lutscher (2023) in integrodifference models. Such anomalous spreading was also observed in the results of Elliott and Cornell (2012) and Morris et al. (2019). These two studies focused on the impact of varying growth rate R and diffusion rate D on the spreading speed of a system made up of two morphs, typically an R-specialist (with a high growth rate R^+ and low diffusion rate D^-) and a D-specialist (with a low growth rate $R^- < R^+$ and high diffusion rate $D^+ > D^-$) in a spatially homogeneous environment. They observed that, for some combinations of values of R and D, and with a low mutation rate between the two morphs, the system could spread faster when both morphs were present than when only one morph was present. This unexpected outcome appears to arise from the synergistic effect of the growth rate of the R-specialist and the diffusion rate of the D-specialist during expansion. We also observed an anomalous spreading speed, induced by mutations, and which can be interpreted by the fact that

the population exploits the best morph at each spatial point: viewing mutations as a form of dispersal along a phenotypic dimension, mutations can increase the spreading speed by enabling individuals to spread while they follow a trajectory that winds through, predominantly remaining in the most favorable habitats.

When we observe habitats with minimal fragmentation ($L \to \infty$), there is a discontinuity in speed with respect to the parameter μ at $\mu = 0$. This means that introducing a second morph with reverse specialization leads to a significantly higher speed, even if the mutation rate between the two morphs is very small. An explanation for this result comes from the idea that large host patches favor the selection of specialists that thrive on their preferred hosts (Papaix et al., 2013). Therefore, the mutation rate should be greater than 0 to allow the emergence of each morph in each newly colonized patch but as small as possible to minimize the mutation load from the appearance of ill-adapted morphs. From a mechanistic perspective, when a morph that is well-adapted to its current patch arrives in a new patch, it takes some time to switch to the other morph. This switching time should depend on the local conditions at the beginning of the new patch and go to infinity as $\mu \to 0$. Thus, for finite L, when μ is too small, mutating to the other morph with the right specialization becomes useless in terms of speed, and the mutation load also becomes negligible. The system therefore behaves as in the one-morph case, leading to the continuity of the speed at $\mu = 0$. However, for each fixed small μ, when L is large enough, the switching time becomes negligible compared to the overall time it takes to cross the new patch with the highest growth rate. In particular, as $L \to \infty$, the impact of the switching time on the spreading speed vanishes, which explains the discontinuity of $c^{2m}(L \to \infty)$ at $\mu = 0$.

Given that $c^{2\,m}$ is an increasing function of the period L, as observed in our numerical simulations, our results encompass the entire spectrum of spreading speed variation, contingent on environmental fragmentation. This range can be quantified analytically by the difference between $c^{2\,m}(L \to \infty)$ and $c^{2\,m}(L \to 0)$, thereby offering a quantitative measure of the potential impact of the fragmentation: it decreases as μ increases and is maximal as $\mu \to 0$. In this limiting scenario, the potential impact of the fragmentation amounts to $2\sqrt{D\,R^+} - \sqrt{2\,D\,(R^+ + R^-)}$. Therefore, it is much more important than in the one-morph setting (or $\mu = 0$). The cultivation of mixtures of susceptible ($R^+ > 0$) and resistant ($R^- = 0$) cultivars has been extensively studied in the literature (Mundt, 2002; Borg et al., 2018; Rimbaud et al., 2021). While several studies have highlighted the role of spatial structure among host genotypes in influencing disease spread (Papaix et al., 2014; Skelsey et al., 2005), our results suggest that in scenarios where pathogens can adapt to different hosts, landscape configuration significantly influences the outcome. Therefore, landscape design can play a pivotal role in efforts to slow down pathogen spread.

Our results on the optimal value of the mutation parameter μ illustrate the dual nature of the impact of mutations on the spreading speed with respect to the fragmentation of the environment: (i) mutations allow the population to adapt to new environments, proving beneficial in highly fragmented settings (small L), while (ii) mutations can also give rise to a large mutation load, resulting in recurrent introduction of ill-adapted phe-

notypes, leading to decreased speeds in less fragmented environments (large L). This can also be interpreted through the trade-off between generalist and specialist morphs. It has been established that high migration rates between two patches (Débarre and Gandon, 2010) or highly fragmented environments (Papaix et al., 2013) tend to favor generalist strategies. These strategies correspond to populations that are moderately adapted to both patches. Here, in highly fragmented environments, a higher optimal value of the mutation parameter μ appears to suggest the same principle, as the limit $\mu \to \infty$ yields the same results as a one-morph model with averaged parameters (refer to the following paragraph for details). As fragmentation decreases, specialists are favored, and the value of μ that optimizes the spreading speed decreases towards 0 as $L \to \infty$.

For clarity and to achieve simpler formulas, we only considered a scenario where the growth rates of the two morphs mirror each other ($r^u = R^+$ when $r^v = R^-$ and vice versa). However, the methodology introduced in this study paves the way for more complex situations, such as when R^+ and R^- have different values depending on the morph. First, when $L \to 0$, the system behaves as if r^u and r^v were replaced by their respective spatial averages. When $\mu \to \infty$, the ability of persistence and the spreading speed behave as if the growth rates r^u and r^v at each spatial point x were replaced by their averaged value $(r^u(x) + r^v(x))/2$. Thus in the case where $r^u = R^+$ when $r^v = R^-$ and vice versa, the two limits coincide; but this has no reason to be true in general. Second, we also proposed a conjecture for the limiting spreading speed in cases of minimal fragmentation ($L \to \infty$) with general growth rates and potentially different diffusion terms between morphs. This formula suggests that our result (9) for the spreading speed in low-fragmented environments is valid under slightly more general assumptions. Additionally, it could allow future works to consider other scenarios than the interaction between two specialist morphs, for example, the case of a specialist morph associated with a generalist, or the case of a D-specialist paired with an R-specialist, as seen in Elliott and Cornell (2012) and Morris et al. (2019), but in the presence of spatial heterogeneities (see some calculations in Appendix C).

Several other assumptions of this work could be revisited, and numerous extensions are conceivable. Among these, we discuss below the consideration of an Allee effect, of discontinuities at the patch interfaces, and the inclusion of a continuous set of morphs. Among these, we discuss below what happens if one takes into account an Allee effect, discontinuities at the patch interfaces, or if one considers a continuous set of morphs.

First, we worked in the absence of an Allee effect (a positive relationship between individual fitness and population density at low densities, Allee, 1931). Although the Allee effect is identified in numerous organisms and can result from various co-occurring processes (Berec et al., 2007), the combination of an Allee effect and evolutionary mechanisms is relatively rare in the literature (but see Lutscher et al., 2023). We expect that the dependency profile between $c^{2\,m}$ and μ will be fundamentally different, especially with a strong Allee effect (negative growth rate at low densities), due to the stability of the steady state 0 (no hair-trigger effect). Compared to $\mu = 0$, a small mutation rate would only slow down the spreading by creating a load without creating a

critical mass that allows the other morph to propagate. For larger values of μ, the ability to mutate to a more adapted morph could avoid blocking phenomena (zero speed) that arise in a heterogeneous environment and with a single morph (or with $\mu = 0$) in the presence of an Allee effect (Keitt et al., 2001; Hamel et al., 2010; Wang et al., 2019). The methods developed in this manuscript, which are mainly based on the analysis of principal eigenvalues of linear operators, however, will not be applicable. Although there is no general formula for the spreading speed in the presence of an Allee effect, homogenization techniques can be used to obtain approximate expressions (Maciel and Lutscher, 2015). Recently, Ding et al. (2022) obtained a limit speed as $L \to \infty$ in the one-morph case with a strong Allee effect. With a two-patch environment, and under conditions that guarantee the spreading in each homogeneous environment, it is simply given as the harmonic mean of the speeds associated with each homogeneous environment. Their methods, in the limit $L \to \infty$, could potentially be extended to study the spreading speed for a two-morph model with an Allee effect.

Second, given that each morph is specialized for a specific host, it would be natural to reevaluate our findings by considering a preference for certain types of patches in individual movements – specifically, minimal migration from favorable to unfavorable patches and vice versa, accompanied by variable diffusion rates that depend on both the patch and the morph. These factors challenge the usual assumption that population densities are continuous across patch interfaces. To reexamine this hypothesis, one could build upon the research conducted in single-species models by Maciel and Lutscher (2013) and Yurk and Cobbold (2018), where a formula for the spreading speed in scenarios with small periodic variations has been established, and homogenization techniques have been developed.

Last, although the two-morph system has allowed us to identify certain key aspects related to the interactions between spatial heterogeneities and adaptation, in many real situations, mutations can lead to a multitude of morphs. An extension of our work is to consider, as in the approaches of Alfaro et al. (2013, 2017); Peltier (2020); Alfaro and Peltier (2022), a population structured in space, via the variable x, and in phenotypic traits, via another variable θ, and to assume a diffusive effect of mutations on phenotypes, leading to a model of the form:

$$\partial_t u(t,x,\theta) = D\partial_{xx} u + \mu \partial_{\theta\theta} u + r_L(x,\theta)u - u \int u(t,x,s)\, ds, \tag{11}$$

where $r_L(x,\theta)$ is again $L-$periodic in x, and describes the suitability of the phenotype θ to the local condition. A major technical challenge will be to show that there is an asymptotic spreading speed and that this speed satisfies a Freidlin-Gärtner formula of the form (6). As in the present study, we can then examine the various limits $L \to 0$, $L \to \infty$, $\mu \to 0$ and $\mu \to \infty$ to get more explicit insight into the intertwined effects of spatial heterogeneities and adaptation.

Appendix A. Population persistence, proofs of the results of Table 1.

Theorem 2.9 of Griette and Matano (2021) shows that a necessary and sufficient condition for persistence is $k_0^{2\,m} > 0$, where $k_0^{2\,m}$ is the principal eigenvalue of the operator $\mathcal{L}_0^{2\,m}$:

$$\mathcal{L}_0^{2\,m}:\ (\phi_1,\phi_2)\mapsto (D\phi_1''+r_L^u(x/L)\phi_1+\mu(\phi_2-\phi_1), D\phi_2''+r_L^v(x/L)\phi_2+\mu(\phi_1-\phi_2))$$

with periodicity conditions. In other words, there is a pair of positive principal eigenfunctions (ϕ_1,ϕ_2) satisfying $\mathcal{L}_0^{2\,m}(\phi_1,\phi_2)=(k_0^{2\,m}\,\phi_1,\ k_0^{2\,m}\,\phi_2)$ with periodicity conditions. Setting $(\psi_1,\psi_2)(x)=(\phi_1,\phi_2)(L\,x)$ one may also write:

$$\begin{cases} \frac{D}{L^2}\psi_1''+R^+\psi_1+\mu(\psi_2-\psi_1)= & k_0^{2\,m}\psi_1,\\ \frac{D}{L^2}\psi_2''+R^-\psi_2+\mu(\psi_1-\psi_2)= & k_0^{2\,m}\psi_2, \end{cases} \text{ in } [0,1/2) \tag{A.1}$$

and

$$\begin{cases} \frac{D}{L^2}\psi_1''+R^-\psi_1+\mu(\psi_2-\psi_1)= & k_0^{2\,m}\psi_1,\\ \frac{D}{L^2}\psi_2''+R^+\psi_2+\mu(\psi_1-\psi_2)= & k_0^{2\,m}\psi_2, \end{cases} \text{ in } [1/2,1), \tag{A.2}$$

where ψ_1, ψ_2 are 1-periodic.

The following Rayleigh formula is also available:

$$k_0^{2\,m}=\max_{(\psi_1,\psi_2)\in E} Q(\psi_1,\psi_2), \tag{A.3}$$

where

$$Q(\psi_1,\psi_2):=-\frac{D}{L^2}\int_0^1[(\psi_1')^2+(\psi_2')^2]+\int_0^1(r^u\,\psi_1^2+r^v\,\psi_2^2)+\mu\left(2\int_0^1\psi_1\,\psi_2-1\right), \tag{A.4}$$

and

$$E:=\left\{(\psi_1,\psi_2)\in H^1_{per}(\mathbb{R})^2,\ \int_0^1\psi_1^2+\psi_2^2=1\right\}$$

and $H^1_{per}(\mathbb{R})$ is the subspace of the Sobolev space $H^1_{loc}(\mathbb{R})$, made of $1-$periodic functions.

For completeness, we also recall the criterion for persistence in the case of a unique morph governed by the equation $\partial_t u(t,x)=d\,\partial_{xx}u+r_L^u(x)\,u-\gamma_L(x)\,u^2$ (see Berestycki et al., 2005a). In this case, the criterion is $k_0^{1\,m}>0$, where $k_0^{1\,m}$ is the principal eigenvalue of the operator $\mathcal{L}_0^{1\,m}$: $(\psi,\psi_2)\mapsto\frac{D}{L^2}\psi_1''+r_L^u(x)\psi$ with periodicity conditions. This principal eigenvalue can be characterized by the Rayleigh formula:

$$k_0^{1\,m}=\max_{\psi\in G}\left(-\frac{D}{L^2}\int_0^1(\psi')^2+\int_0^1 r^u\,\psi^2\right),$$

with $G:=\left\{\psi\in H^1_{per}(\mathbb{R}),\ \int_0^1\psi^2=1\right\}$.

Arbitrary μ, with $L \to 0$. Taking two constant functions $\psi_1 = \psi_2 = 1/\sqrt{2}$, we note that $Q(\psi_1, \psi_2) = \int_0^1 r^u + r^v = (R^+ + R^-)/2$. Thus (A.3) implies that $k_0^{2\,m} \geq (R^+ + R^-)/2$. Conversely, as $L \to 0$, due to the first term in (A.4), the functions ψ_1, ψ_2 that realize the maximum in (A.3) necessarily converge to constants. Maximizing Q over the pairs of constant functions in E, we conclude that $\lim_{L\to 0} k_0^{2\,m} = (R^+ + R^-)/2$. This expression is independent of μ, and therefore remains unchanged if we pass to the limit $\mu \to 0$ or $\mu \to \infty$.

Arbitrary μ, with $L \to \infty$. Passing to the limit $L \to \infty$ in (A.1)-(A.2) means solving the system

$$\begin{cases} a\,R^+ + \mu(b-a) = & \left(\lim\limits_{L\to+\infty} k_0^{2\,m}\right) a, \\ b\,R^- + \mu(a-b) = & \left(\lim\limits_{L\to+\infty} k_0^{2\,m}\right) b, \end{cases} \tag{A.5}$$

with $a, b > 0$. This leads to:

$$\lim_{L\to\infty} k_0^{2\,m} = \frac{1}{2}\sqrt{(R^+ - R^-)^2 + 4\,\mu^2} - \mu + (R^+ + R^-)/2.$$

To determine when persistence holds, we solve $\lim\limits_{L\to\infty} k_0^{2\,m} > 0$, which is equivalent to

$$\sqrt{(R^+ - R^-)^2 + 4\,\mu^2} > 2\mu - (R^+ + R^-).$$

This always holds if $R^+ + R^- > 0$. If $R^+ + R^- < 0$ (so $R^+ > 0 > R^-$), this becomes:

$$R^+ > \frac{\mu}{1 + (\mu/(-R^-))}.$$

If we pass to the limit $\mu \to 0$, this condition becomes $R^+ > 0$, and if we pass to the limit $\mu \to \infty$, this condition becomes $R^+ + R^- > 0$.

Arbitrary L, with $\mu \to 0$. We denote by (ψ_1^μ, ψ_2^μ) the principal eigenfunctions in (A.1)-(A.2) and $k_0^\mu := k_0^{2\,m}$ the associated principal eigenvalue. We have:

$$\frac{D}{L^2}(\psi_1^\mu)'' + r^u(x)\psi_1^\mu + \mu(\psi_2^\mu - \psi_1^\mu) = k_0^\mu \psi_1^\mu.$$

The functions ψ_1^μ and ψ_2^μ are bounded. Using the so-called Schauder estimates, we obtain that as $\mu \to 0$, the functions ψ_1^μ and ψ_2^μ converge to functions ψ_1^0 and ψ_2^0 in a strong sense. Thus, taking $\mu \to 0$, the mutation term disappears and we obtain:

$$\frac{D}{L^2}(\psi_1^0)'' + r^u(x)\psi_1^0 + = k_0^0 \psi_1^0,$$

which is precisely the eigenvalue problem defining $k_0^{1\,m}$. Thus

$$\lim_{\mu\to 0} k_0^\mu = k_0^{1\,m}.$$

If we pass to the limit $L \to 0$, this leads to the condition for persistence $R^+ + R^- > 0$, and with $\mu \to 0$, this leads to the condition for persistence $R^+ > 0$.

Arbitrary L, with $\mu \to \infty$. With the same notations as in the previous paragraph, multiplying by ψ_1^μ the equation satisfied by ψ_1^μ and integrating by parts, we get:

$$-\frac{D}{L^2}\int_0^1 ((\psi_1^\mu)')^2 + \mu\int_0^1 (\psi_2^\mu - \psi_1^\mu)\psi_1^\mu = \int_0^1 k_0^\mu (\psi_1^\mu)^2 - \int_0^1 r^u(x)(\psi_1^\mu)^2. \tag{A.6}$$

Without loss of generality, we can assume that $\int_0^1 (\psi_1^\mu)^2 = 1$, and using the upper bound for k_0^μ obtained above (in the limit $L \to \infty$), we get that the right-hand side in (A.6) is bounded independently of μ. Moreover, by uniqueness and symmetry of the eigenvalue problem, we have $\psi_2^\mu(x) = \psi_1^\mu(1-x)$ for all x. Thus, the Cauchy-Schwarz inequality implies that the integral $\int_0^1 (\psi_2^\mu - \psi_1^\mu)\psi_1^\mu$ is negative. As the other term in the left-hand side of (A.6) is negative, and the right-hand side is bounded, this implies that, as $\mu \to \infty$,

$$\int_0^1 (\psi_2^\infty - \psi_1^\infty)\psi_1^\infty(x)\,dx = 0.$$

Since both functions ψ_1^∞ and $\psi_2^\infty(\cdot) = \psi_1^\infty(1-\cdot)$ are positive and share the same L^2 norm, the Cauchy-Schwarz inequality implies that $\psi_1^\infty(\cdot) \equiv \psi_2^\infty(\cdot)$. In other words, $\psi_1^\mu - \psi_2^\mu \to 0$. Adding the two lines (A.1)-(A.2), we obtain:

$$\frac{D}{L^2}(\psi_1^\mu + \psi_2^\mu)'' + r^u(x)\psi_1^\mu + r^v(x)\psi_2^\mu = k_0^\mu(\psi_1^\mu + \psi_2^\mu).$$

Thus, taking $\mu \to \infty$ in the last equation gives:

$$\frac{D}{L^2}(2\psi_1^\infty)'' + (R^+ + R^-)\psi_1^\infty = 2\,k_0^\infty\,\psi_1^\infty.$$

Therefore, the principal eigenfunction ψ_1^∞ is constant and the corresponding principal eigenvalue is

$$\lim_{\mu\to\infty} k_0^\mu = \frac{R^+ + R^-}{2}.$$

This formula is independent of L, and therefore remains unchanged if we pass to the limit $L \to 0$ or $L \to \infty$.

Appendix B. Spreading speed, proofs of the results of Table 2.

Arbitrary L, with $\mu \to 0$. We denote by (ψ_1^μ, ψ_2^μ) the solution of the principal eigenvalue problem (7) and we let k_λ^μ be the associated principal eigenvalue. We focus on the first line:

$$(D\psi_1^\mu)'' + 2\lambda\,D\,(\psi_1^\mu)' + (\lambda^2\,D + r_L^u(x))\psi_1^\mu + \mu(\psi_2^\mu - \psi_1^\mu) = k_\lambda^\mu\psi_1^\mu. \tag{B.1}$$

The functions ψ_1^μ and ψ_2^μ are bounded. Using the so-called Schauder estimates, we obtain that as $\mu \to 0$, the functions ψ_1^μ and ψ_2^μ converge to functions ψ_1^0 and ψ_2^0 in

a strong sense. Thus, taking $\mu \to 0$ in (B.1), the mutation term disappears and we obtain:

$$(D\psi_1^0)'' + 2\lambda\, D\,(\psi_1^0)' + (\lambda^2\, D + r_L^u(x))\psi_1^0 = k_\lambda^0 \psi_1^0.$$

This is precisely the eigenvalue problem defining $k_\lambda^{1\,m}$, such that the spreading speed with a unique morph with growth rate r_L^u is given by the Freidlin-Gärtner formula (e.g. Berestycki et al., 2005)

$$c^{1\,m} = \min_{\lambda>0} \frac{k_\lambda^{1\,m}}{\lambda}.$$

Thus

$$\lim_{\mu\to 0} c^{2\,m} = c^{1\,m}.$$

The limits $L \to 0$ and $L \to \infty$ therefore correspond to the known limits in the one-morph setting, see (El Smaily et al., 2009) and (Hamel et al., 2010).

Arbitrary L, with $\mu \to \infty$. We use the same notations as the previous paragraph. Multiplying by ψ_1^μ the equation satisfied by ψ_1^μ and integrating by parts, we get:

$$-D\int_0^L ((\psi_1^\mu)')^2 + \mu\int_0^L (\psi_2^\mu - \psi_1^\mu)\psi_1^\mu = \int_0^L k_\lambda^\mu (\psi_1^\mu)^2 - \int_0^L (\lambda^2\, D + r^u(x))(\psi_1^\mu)^2. \quad \text{(B.2)}$$

Without loss of generality, we can assume that $\int_0^L (\psi_1^\mu))^2 = 1$, and Lemma 1 implies that the right-hand side in (B.2) is bounded independently of μ. Moreover, by uniqueness and symmetry of the eigenvalue problem, we have $\psi_2^\mu(x) = \psi_1^\mu(L-x)$ for all x. Thus, the Cauchy-Schwarz inequality implies that the integral $\int_0^L (\psi_2^\mu - \psi_1^\mu)\psi_1^\mu$ is negative. As the other term in the left-hand side of (B.2) is negative, and the right-hand side is bounded, this implies that, as $\mu \to \infty$,

$$\int_0^L (\psi_2^\infty - \psi_1^\infty)\psi_1^\infty(x)\, dx = 0.$$

Since both functions ψ_1^∞ and $\psi_2^\infty(\cdot) = \psi_1^\infty(L-\cdot)$ are positive and share the same L^2 norm, Cauchy-Schwarz inequality implies that $\psi_1^\infty(\cdot) \equiv \psi_2^\infty$. In other words, $\psi_1^\mu - \psi_2^\mu \to 0$.

Adding the two lines of (7), we obtain:

$$D(\psi_1^\mu + \psi_2^\mu)'' + 2\lambda\, D\,(\psi_1^\mu + \psi_2^\mu)' + \lambda^2\, D\,(\psi_1^\mu + \psi_2^\mu) + r^u(x)\psi_1^\mu + r^v(x)\psi_2^\mu = k_\lambda^\mu(\psi_1^\mu + \psi_2^\mu).$$

Therefore, as $\mu \to +\infty$,

$$(2D\psi_1^\infty)'' + 2\lambda\, D\,(2\psi_1^\infty)' + \lambda^2\, D\,(2\psi_1^\infty) + (r^u(x) + r^v(x))\psi_1^\infty = k_\lambda^\infty(2\psi_1^\infty).$$

Now note that $r^u(x) + r^v(x) = R^+ + R^-$ is constant. Therefore, the principal eigenfunction ψ_1^∞ is also constant and the corresponding principal eigenvalue is

$$k_\lambda^\infty = \lim_{\mu\to\infty} k_\lambda^\mu = \lambda^2\, D + \frac{R^+ + R^-}{2}.$$

Using the Freidlin-Gärtner formula (6), we get:

$$\lim_{\mu\to\infty} c^{2\,m} = \inf_{\lambda>0}\left(\lambda D + \frac{R^+ + R^-}{2\lambda}\right) = \sqrt{2D(R^+ + R^-)}.$$

This formula is independent of L, and therefore remains unchanged if we pass to the limit $L \to 0$ or $L \to \infty$.

Arbitrary μ, with $L \to 0$. The homogenization results in Griette and Matano (2021) (Theorem 2.20) show that the spreading speed $c^{2\,m}$ converges to the speed that would be obtained in a homogeneous environment where r_L^u and r_L^v would be replaced by their spatial average $(R^+ + R^-)/2$. In this last case, the solution of the eigenvalue problem (7) is a constant eigenfunction and the eigenvalue is $k_\lambda^0 = \lambda^2 D + (R^+ + R^-)/2$. Using the Freidlin-Gärtner formula (6), we get:

$$\lim_{L\to 0} c^{2\,m} = \inf_{\lambda>0}\left(\lambda D + \frac{R^+ + R^-}{2\lambda}\right) = \sqrt{2D(R^+ + R^-)}.$$

This formula is independent of μ, and therefore remains unchanged if we pass to the limit $\mu \to 0$ or $\mu \to \infty$.

Arbitrary μ, with $L \to \infty$. This is the most involved case. We set

$$I_L := \left(\frac{\sqrt{(R^+ - R^-)/2}}{\sqrt{D}}, \frac{\sqrt{R^+} + \sqrt{(R^+ - R^-)/2}}{\sqrt{D}}\right). \tag{B.3}$$

We begin by considering values of λ in I_L.

Let us set $(\varphi_1(x), \varphi_2(x)) = (e^{\lambda x}\,\phi_1(x), e^{\lambda x}\,\phi_2(x))$. The system (7) becomes

$$\begin{cases} D\varphi_1'' + r_L^u(x)\varphi_1 + \mu(\varphi_2 - \varphi_1) = & k_\lambda\varphi_1, \\ D\varphi_2'' + r_L^u(x)\varphi_2 + \mu(\varphi_1 - \varphi_2) = & k_\lambda\varphi_2, \end{cases} \text{ in } [0, L]. \tag{B.4}$$

Writing this system on each interval where the coefficients are constants, we get:

$$\begin{cases} D\varphi_1'' + R^+\varphi_1 + \mu(\varphi_2 - \varphi_1) = & k_\lambda\varphi_1, \\ D\varphi_2'' + R^-\varphi_2 + \mu(\varphi_1 - \varphi_2) = & k_\lambda\varphi_2, \end{cases} \text{ in } [0, L/2), \tag{B.5}$$

$$\begin{cases} D\varphi_1'' + R^-\varphi_1 + \mu(\varphi_2 - \varphi_1) = & k_\lambda\varphi_1, \\ D\varphi_2'' + R^+\varphi_2 + \mu(\varphi_1 - \varphi_2) = & k_\lambda\varphi_2, \end{cases} \text{ in } [L/2, L). \tag{B.6}$$

The functions φ_1, φ_2 are of class C^1 on the whole space $\mathbb{R}$, and are of class C^2 on the intervals $(k, k + L/2)$ and $(k + L/2, k + L)$, $k \in \mathbb{Z}$, i.e., on the intervals where the coefficients are constant. Without loss of generality, as the pair $(\varphi_1(x), \varphi_2(x))$ is defined

up to a multiplicative constant, we may set $\varphi_1(0) = 1$. Altogether, with the periodicity and regularity conditions, we obtain the following constraints:

$$\begin{cases} \varphi_2(L) &= e^{\lambda L}\varphi_2(0), \\ \varphi_1'(L) &= e^{\lambda L}\varphi_1'(0), \\ \varphi_2'(L) &= e^{\lambda L}\varphi_2'(0), \\ \lim\limits_{s\to(L/2)^-} \varphi_1(s) &= \lim\limits_{s\to(L/2)^+} \varphi_1(s), \\ \lim\limits_{s\to(L/2)^-} \varphi_2(s) &= \lim\limits_{s\to(L/2)^+} \varphi_2(s), \\ \lim\limits_{s\to(L/2)^-} \varphi_1'(s) &= \lim\limits_{s\to(L/2)^+} \varphi_1'(s), \\ \lim\limits_{s\to(L/2)^-} \varphi_2'(s) &= \lim\limits_{s\to(L/2)^+} \varphi_2'(s), \end{cases} \tag{B.7}$$

and another constraint that we will treat separately:

$$\varphi_1(L) = e^{\lambda L}\varphi_1(0) = e^{\lambda L}. \tag{B.8}$$

We directly solve the two systems (B.5) and (B.6) of two constant coefficient second order linear homogeneous differential equations. Their general solution can be found, e.g., in Kamke (2013). The characteristic equation has the form:

$$X^4 - [(2k_\lambda + 2\mu - R^+ - R^-)/D]X^2 + (k_\lambda + \mu - R^+)(k_\lambda + \mu - R^-)/D^2 - \mu^2/D^2 = 0.$$

Under the conditions $(k_\lambda + \mu - R^+)(k_\lambda + \mu - R^-) - \mu^2 \neq 0$ (which follows from $\lambda \in I_L$, see Lemma 3) and $(R^+ - R^-)^2 + 4\,\mu^2 \neq 0$ (which is always satisfied), the characteristic equation has four distinct roots $\pm Z_1$ and $\pm Z_2$, with:

$$\begin{cases} \delta &:= \sqrt{(R^+ - R^-)^2 + 4\,\mu^2}, \\ Z_1 &:= \sqrt{\dfrac{2\mu + 2k_\lambda - \delta - R^+ - R^-}{2D}}, \\ Z_2 &:= \sqrt{\dfrac{2\mu + 2k_\lambda + \delta - R^+ - R^-}{2D}}. \end{cases} \tag{B.9}$$

The solutions of (B.5) with the constraint $\varphi_1(0) = 1$ are, for $x \in (0, L/2)$,

$$\begin{cases} \varphi_1(x) &= (1 - A_1 - A_2 - A_3)e^{-Z_1\,x} + A_1 e^{Z_1\,x} + A_2 e^{-Z_2\,x} + A_3 e^{Z_2\,x}, \\ \varphi_2(x) &= \dfrac{R^- - R^+ + \delta}{2\,\mu}\left[(1 - A_1 - A_2 - A_3)e^{-Z_1\,x} + A_1\,e^{Z_1\,x}\right] \\ &\quad + \dfrac{R^- - R^+ - \delta}{2\,\mu}\left[A_2 e^{-Z_2\,x} + A_3 e^{Z_2\,x}\right], \end{cases} \tag{B.10}$$

with $A_1, A_2, A_3 \in \mathbb{R}$. Lemma 2 shows that $2\mu + 2k_\lambda - \delta - R^+ - R^- > 0$, which implies that Z_1, Z_2 are real.

Similarly, the solutions of (B.6) are, for $x \in (L/2, L)$,

$$\left\{ \begin{array}{rcl} \varphi_1(x) & = & A_4\, e^{-Z_1\, x} + A_5 e^{Z_1\, x} + A_6 e^{-Z_2\, x} + A_7 e^{Z_2\, x}, \\ \varphi_2(x) & = & \dfrac{R^+ - R^- + \delta}{2\,\mu} \left[A_4 e^{-Z_1\, x} + A_5\, e^{Z_1\, x} \right] + \dfrac{R^+ - R^- - \delta}{2\,\mu} \left[A_6 e^{-Z_2\, x} + A_7 e^{Z_2\, x} \right], \end{array} \right. \tag{B.11}$$

with $A_4, A_5, A_6, A_7 \in \mathbb{R}$.

Plugging the constraints (B.7) in (B.10) and (B.11), we observe that the coefficients $A_1, \ldots, A_7$ solve a linear system with 7 equations, for which we obtain an explicit solution which leads to explicit (but very lengthy) expressions for φ_1 and φ_2. Using $Z_1 < Z_2$, one may then write the last constraint (B.8) in the form

$$\begin{aligned} & B_1 e^{L(2Z_1+2Z_2+3\lambda)} - B_2 e^{L(2Z_1+Z_2+4\lambda)} - B_3 e^{L(3Z_1+2Z_2+2\lambda)} \\ & + o(B_1 e^{L(2Z_1+2Z_2+3\lambda)} + B_2 e^{L(2Z_1+Z_2+4\lambda)} + B_3 e^{L(3Z_1+2Z_2+2\lambda)}) = 0, \text{ as } L \to \infty, \end{aligned} \tag{B.12}$$

where $B_1, B_2, B_3 > 0$ are bounded independently of L. See Supplementary Maple notebook (pdf file available as Supplementary Material and code available at `https://doi.org/10.17605/OSF.IO/7RTFK`).

Let us show that the term $\exp[L(3Z_1 + 2Z_2 + 2\lambda)]$ dominates $\exp[L(2Z_1 + Z_2 + 4\lambda)]$ as $L \to \infty$. Assume by contradiction that there exists $C > 0$ such that for all $L > 0$, we have $\exp[L(2Z_1 + Z_2 + 4\lambda)] \geq C \exp[L(3Z_1 + 2Z_2 + 2\lambda)]$. Then, using (B.12), we get that $2Z_1 + 2Z_2 + 3\lambda \sim 2Z_1 + Z_2 + 4\lambda$ which implies that:

$$\lim_{L\to\infty} Z_2 = \lambda. \tag{B.13}$$

Coming back to the expression of Z_2 in (B.9), and setting $k_\lambda^\infty := \lim_{L\to\infty} k_\lambda$, this shows that $k_\lambda^\infty = \lambda^2\, D + (R^+ + R^- - \delta)/2 - \mu$. Thus, $k_\lambda^\infty < \lambda^2\, D + (R^+ + R^-)/2$, which is in contradiction with the lower bound in Lemma 1. Thus, $\exp[L(3Z_1 + 2Z_2 + 2\lambda)]$ dominates $\exp[L(2Z_1 + Z_2 + 4\lambda)]$ as $L \to \infty$ and, with (B.12), we necessarily get $2Z_1 + 2Z_2 + 3\lambda \sim 3Z_1 + 2Z_2 + 2\lambda$. This implies that:

$$\lim_{L\to\infty} Z_1 = \lambda. \tag{B.14}$$

Using the expression of Z_1 in (B.9), this shows that

$$k_\lambda^\infty = \lambda^2\, D + \frac{1}{2}(R^+ + R^- + \delta) - \mu. \tag{B.15}$$

We note that this expression is consistent with the result of Lemma 1. We observe that $\lambda \mapsto k_\lambda^\infty$ is convex in I_L and that $\lambda \mapsto k_\lambda^\infty/\lambda$ reaches a (strict) minimum in I_L at $\lambda_m = \sqrt{(R^+ + R^- + \delta - 2\mu)/(2D)}$. From Proposition 2.2 in Griette and Matano (2021), we also know that $\lambda \mapsto k_\lambda$ is strictly convex in $\mathbb{R}^+$. Thus $\lambda \mapsto k_\lambda^\infty$ is convex in $\mathbb{R}^+$. This implies that k_λ^∞/λ reaches its (unique) strict minimum in I_L at $\lambda = \lambda_m$ (this

is easily seen graphically, as k_λ^∞/λ reaches its minimum in $\mathbb{R}^+$ at values of λ such that $k_\lambda^\infty = \lambda\,\partial_\lambda(k_\lambda^\infty))$. Finally, this shows that

$$\lim_{L\to\infty} c^{2\,m} = \min_{\lambda>0} \frac{k_\lambda^\infty}{\lambda} = \min_{\lambda\in I_L} \frac{k_\lambda^\infty}{\lambda} = \sqrt{2D\left(R^+ + R^- + \sqrt{(R^+ - R^-)^2 + 4\,\mu^2} - 2\mu\right)}. \tag{B.16}$$

Using this formula, we readily obtain the limits:

$$\lim_{\mu\to 0}\lim_{L\to\infty} c^{2\,m} = 2\sqrt{D\,R^+} \text{ and } \lim_{\mu\to\infty}\lim_{L\to\infty} c^{2\,m} = \sqrt{2\,D\,(R^+ + R^-)}.$$

Appendix C. A conjecture for a general formula for the speed

We would like to adapt to our context the results of Hamel et al. (2011), who dealt with the limit as $L \to \infty$ of the spreading speed when there is only one morph. For simplicity we assume that the diffusion coefficient is $D = 1$.

In the one-morph setting, Hamel et al. (2011) showed that the limit of the spreading speed as $L \to +\infty$ is

$$c^{1\,m}(L \to +\infty) = \inf_{\lambda>0} \frac{\bar{j}^{-1}(\lambda)}{\lambda},$$

where

$$\bar{j}(k) = \int_0^1 \sqrt{k - r(x)}dx,$$

Here, r plays the role of r^u and r^v. If we adapt their calculations to our case, we find the same expression for the limiting speed $c^{2\,m}$, but $\bar{j}(k)$ is replaced by

$$j(k) = \int_0^1 \sqrt{k - \left(r^u(x) - \mu + \mu\frac{\psi_{2,\infty}(x)}{\psi_{1,\infty}(x)}\right)}dx. \tag{C.1}$$

Here, the functions $\psi_{1,\infty}$ and $\psi_{2,\infty}$ are defined as the limits as $L \to \infty$ of the principal eigenfunctions $\psi_{1,L}(x) = \phi_{1,L}(Lx)$ and $\psi_{2,L} = \phi_{2,L}(Lx)$:

$$\psi_{1,\infty}(x) := \lim_{L\to\infty} \psi_{1,L}(x), \qquad \psi_{2,\infty}(x) := \lim_{L\to\infty} \psi_{2,L}(x).$$

The extra term $-\mu + \mu\frac{\psi_{2,\infty}}{\psi_{1,\infty}}$ arises because of the mutations between morphs. The hard part is to compute the value of $\frac{\psi_{2,\infty}}{\psi_{1,\infty}}$. Let us first assume that r^u and r^v are constant (i.e., the environment is homogeneous): $r^u(x) \equiv r^u$ and $r^v(x) \equiv r^v$. Then the eigenfunctions ψ_1 and ψ_2 are independent of x, so the system (7) becomes:

$$\begin{cases} -(r^u - \mu + \lambda^2)\psi_1 - \mu\psi_2 = k_\lambda\psi_1 \\ -(r^v - \mu + \lambda^2)\psi_2 - \mu\psi_1 = k_\lambda\psi_2, \end{cases}$$

where ψ_1 and ψ_2 are real numbers (instead of functions). Solving this system, with the constraints that $\psi_1 > 0$ and $\psi_2 > 0$, yields:

$$\frac{\psi_{2,\infty}}{\psi_{1,\infty}} = \frac{1}{2\mu}\left(r^v - r^u + \sqrt{(r^u - r^v)^2 + 4\mu^2}\right).$$

Then, when r^u and r^v are constant, the expression of j (C.1) becomes:

$$j(k) := \int_0^1 \sqrt{k - \frac{1}{2}\left[r^u + r^v - 2\mu + \sqrt{(r^u - r^v)^2 + 4\mu^2}\right]}dx. \tag{C.2}$$

Now we would like to extend this result to the case when r^u and r^v are not necessarily constant. In fact, as the period grows, the environment becomes more and more homogeneous. This suggests that the expression (C.2) of j, which holds when r^u and r^v are constant, should also hold for nonconstant r^u and r^v. This is the following conjecture. Let us write

$$j(k) := \int_0^1 \sqrt{k - \frac{1}{2}\left[r^u(x) + r^v(x) - 2\mu + \sqrt{(r^u(x) - r^v(x))^2 + 4\mu^2}\right]}dx.$$

Then

$$c^{2\,m}(L \to \infty) = \inf_{\lambda > 0} \frac{j^{-1}(\lambda)}{\lambda}.$$

This expression generalises the one we proved above for the particular form of r^u and r^v that was the main focus of this study. This new general expression is quite complicated, because we need to consider the inverse of the function j. Still, is is possible to find some qualitative properties.

Dependence of the speed on the mutation rate. We are interested in the variations of the speed $c^{2\,m}(L \to \infty)$ in terms of the mutation rate, so we will use the notations $j(k, \mu)$ and $c^{2\,m}(L \to \infty)(\mu)$ for clarity. We have:

$$\frac{\partial}{\partial \mu} j(k, \mu) = \int_0^1 \frac{1 - \frac{2\mu}{2\sqrt{(r^u(x) - r^v(x))^2 + 4\mu^2}}}{2\sqrt{k - \frac{1}{2}\left[r^u(x) + r^v(x) - 2\mu + \sqrt{(r^u(x) - r^v(x))^2 + 4\mu^2}\right]}}dx.$$

Since $\sqrt{(r^u(x) - r^v(x))^2 + 4\mu^2} \geq \sqrt{4\mu^2} = 2\mu$, we conclude that

$$\frac{\partial}{\partial \mu} j(k, \mu) \geq 0.$$

Now, (6) implies that

$$c^{2\,m}(L \to \infty)(\mu) = \inf_k \frac{k}{j(k, \mu)}.$$

We conclude that $\mu \mapsto c^{2\,m}(L \to \infty)(\mu)$ is a nonincreasing function.

When the diffusion terms are different. If the diffusion terms are different for u and v, say D^u and D^v, then our conjecture implies that the formula for j becomes:

$$j(k) := \frac{1}{\sqrt{D^u}} \int_0^1 \sqrt{k - \frac{1}{2}\left[r^u(x) + r^v(x) + \lambda^2 D' - 2\mu + \sqrt{(r^u(x) - r^v(x) + \lambda^2 D')^2 + 4\mu^2}\right]} dx,$$

with $D' = D^v - D^u$. We have not been able to turn this expression into an explicit formula for the spreading speed.

With one specialist and one generalist. Assume that u represents a specialist morph that is well-adapted on $(0, 1/2)$ and ill-adapted on $(1/2, 1)$, and that v represents a generalist morph that is everywhere equally adapted. This can be modeled by replacing the function $r^v(x)$ by a constant $r^v(x) \equiv r^v$, and by letting r^u takes two values R^+ and R^- over $(0, 1/2)$ and $(1/2, 1)$ respectively such that $R^- < r^v < R^+$. Then our conjecture implies that the expression for the speed is:

$$c^{2\,m}(L \to \infty) = \frac{2k_m}{\sqrt{k_m - A} + \sqrt{k_m - B}},$$

where

$$A = \frac{1}{2}\left(R^+ + r^v - 2\mu\sqrt{(R^+ - r^v)^2 + 4\mu^2}\right),$$
$$B = \frac{1}{2}\left(R^- + r^v - 2\mu\sqrt{(R^- - r^v)^2 + 4\mu^2}\right),$$

and

$$k_m = \frac{2}{3}\left(A + B + \sqrt{(A+B)^2 + 3\frac{AB^2 - A^2B}{A - B}}\right).$$

Appendix D. Technical lemmas.

Lemma 1. *For all $\lambda > 0$ and $L > 0$, the principal eigenvalue k_λ in (7) satisfies*

$$\frac{R^+ + R^-}{2} + \lambda^2 D < k_\lambda < R^+ + \lambda^2 D.$$

Proof. First, adding the two equations in (7) and integrating over $(0, L)$, we get:

$$k_\lambda < R^+ + \lambda^2 D. \tag{D.1}$$

Second, dividing the two equations in (7) by ϕ_1 and ϕ_2 respectively, integrating by parts over $(0, L)$, and using the periodicity of ϕ_1, ϕ_2 we get:

$$\left\{\begin{array}{ll} D\displaystyle\int_0^L \frac{|\phi_1'|^2}{\phi_1^2} + \lambda^2 D L + \int_0^L r_L^u(x)dx + \mu\left(\int_0^L \frac{\phi_2}{\phi_1} - L\right) & = k_\lambda L, \\ D\displaystyle\int_0^L \frac{|\phi_2'|^2}{\phi_2^2} + \lambda^2 D L + \int_0^L r_L^v(x)dx + \mu\left(\int_0^L \frac{\phi_1}{\phi_2} - L\right) & = k_\lambda L, \end{array}\right. \quad \text{in } \mathbb{R}. \tag{D.2}$$

Adding the two equations, we obtain:

$$2D\int_0^L\left(\frac{|\phi_1'|^2}{\phi_1^2}+\frac{|\phi_2'|^2}{\phi_2^2}\right)+2\lambda^2\,D\,L+L(R^+{+}R^-)+\mu\left(\int_0^L\left(\frac{\phi_2}{\phi_1}+\frac{\phi_2}{\phi_1}\right)-2L\right)=2k_\lambda\,L. \tag{D.3}$$

Note that $\phi_2/\phi_1+\phi_2/\phi_1\geq 2$ as $\phi_1,\phi_2>0$. Thus

$$k_\lambda>\frac{R^++R^-}{2}+\lambda^2\,D. \tag{D.4}$$

□

Lemma 2. *Let $\lambda\in I_L$ (see* (B.3)*). We have*

$$2\mu+2k_\lambda-\delta-R^+-R^->0.$$

Proof. Using (D.4), we obtain

$$2\mu+2k_\lambda-\delta-R^+-R^->2\mu+2\lambda^2D-\sqrt{(R^+-R^-)^2+4\,\mu^2},$$

and for $\lambda\in I_L$, $2\lambda^2D>R^+-R^-$ so

$$2\mu+2k_\lambda-\delta-R^+-R^->R^+-R^-+2\mu-\sqrt{(R^+-R^-)^2+4\,\mu^2}>0.$$

□

Lemma 3. *Let $\lambda\in I_L$. We have $(k_\lambda-R^++\mu)(k_\lambda-R^-+\mu)-\mu^2\neq 0$.*

Proof. The equation $(k-R^++\mu)(k-R^-+\mu)-\mu^2=0$ admits two roots $k_\pm=\frac{R^++R^-}{2}-\mu\pm\frac{\delta}{2}$. Lemma 2 implies that $k_\lambda>k_+>k_-$, so k_λ cannot be a root of the equation. □

Acknowledgements. This work has received funding from the French ANR RESISTE (ANR-18-CE45-0019).

Author contributions. Lionel Roques: Conceptualization; Formal analysis; Funding acquisition; Methodology; Software; Supervision; Writing - original draft; **Nathanaël Boutillon:** Conceptualization; Formal analysis; Methodology; Software; Writing - original draft; **Patrizia Zamberletti:** Conceptualization; Software; **Julien Papaïx:** Conceptualization; Methodology; Software; Funding acquisition; Supervision; Writing - original draft.

Code availability. All of the codes used in this article are available at `https://doi.org/10.17605/OSF.IO/7RTFK`.

Declarations of interest: none

References

Alfaro, M., H. Berestycki, and G. Raoul (2017). The effect of climate shift on a species submitted to dispersion, evolution, growth, and nonlocal competition. SIAM Journal on Mathematical Analysis 49(1), 562–596.

Alfaro, M., J. Coville, and G. Raoul (2013). Travelling waves in a nonlocal reaction-diffusion equation as a model for a population structured by a space variable and a phenotypic trait. Communications in Partial Differential Equations 38(12), 2126–2154.

Alfaro, M. and G. Peltier (2022). Populations facing a nonlinear environmental gradient: steady states and pulsating fronts. Mathematical Models and Methods in Applied Sciences 32(2), 209–290.

Allee, W. C. (1931). Animal aggregations, a study in general sociology. Chicago: The University of Chicago Press.

Anciaux, Y., A. Lambert, O. Ronce, L. Roques, and G. Martin (2019). Population persistence under high mutation rate: from evolutionary rescue to lethal mutagenesis. Evolution 73(8), 1517–1532.

Aronson, D. G. and H. G. Weinberger (1975). Nonlinear diffusion in population genetics, combustion and nerve propagation. In Partial Differential Equations and Related Topics, Volume 446 of Lectures Notes Math, pp. 5–49. Springer, New York.

Beillouin, D., T. Ben-Ari, E. Malézieux, V. Seufert, and D. Makowski (2021). Positive but variable effects of crop diversification on biodiversity and ecosystem services. Global Change Biology 27(19), 4697–4710.

Berec, L., E. Angulo, and F. Courchamp (2007). Multiple Allee effects and population management. Trends in Ecology & Evolution 22, 185–191.

Berestycki, H., F. Hamel, and G. Nadin (2008). Asymptotic spreading in heterogeneous diffusive excitable media. Journal of Functional Analysis 255(9), 2146–2189.

Berestycki, H., F. Hamel, and N. Nadirashvili (2005). The speed of propagation for KPP type problems. I: Periodic framework. Journal of the European Mathematical Society 7(2), 173–213.

Berestycki, H., F. Hamel, and L. Roques (2005a). Analysis of the periodically fragmented environment model: I - Species persistence. Journal of Mathematical Biology 51(1), 75–113.

Berestycki, H., F. Hamel, and L. Roques (2005b). Analysis of the periodically fragmented environment model: II - Biological invasions and pulsating travelling fronts. Journal de Mathématiques Pures et Appliquées 84(8), 1101–1146.

Borg, J., L. P. Kiær, C. Lecarpentier, I. Goldringer, A. Gauffreteau, S. Saint-Jean, S. Barot, and J. Enjalbert (2018). Unfolding the potential of wheat cultivar mixtures: A meta-analysis perspective and identification of knowledge gaps. Field Crops Research 221, 298–313.

Caquet, T., C. Gascuel, and M. Tixier-Boichard (2020). Agroécologie: des recherches pour la transition des filières et des territoires. Quae.

Cruywagen, G. C., P. Kareiva, M. Lewis, and J. Murray (1996). Comptetition in a spatially heterogeneous environment: Modelling the risk of spread of a genetically engineered population. Theoretical Population Biology 49(1), 1–38.

Débarre, F. and S. Gandon (2010). Evolution of specialization in a spatially continuous environment. Journal of Evolutionary Biology 23(5), 1090–1099.

Débarre, F., O. Ronce, and S. Gandon (2013). Quantifying the effects of migration and mutation on adaptation and demography in spatially heterogeneous environments. Journal of Evolutionary Biology 26(6), 1185–1202.

Ding, W., F. Hamel, and X. Liang (2022). Bistable pulsating fronts in slowly oscillating environments. arXiv preprint arXiv:2204.09301.

El Smaily, M., F. Hamel, and L. Roques (2009). Homogenization and influence of fragmentation in a biological invasion model. Discrete & Continuous Dynamical Systems-A.

Elliott, E. C. and S. J. Cornell (2012). Dispersal polymorphism and the speed of biological invasions. PloS One 7(7), e40496.

Food and Agriculture Organization of the United Nations (2018). The 10 Elements of Agroecology. Guiding the Transition to Sustainable Food and Agricultural Systems. FAO.

Freidlin, M. and J. Gärtner (1979). On the propagation of concentration waves in periodic and random media. Soviet Mathematics - Doklady 20, 1282–1286.

Gascuel-Odoux, C., F. Lescourret, B. Dedieu, C. Detang-Dessendre, P. Faverdin, L. Hazard, I. Litrico-Chiarelli, S. Petit, L. Roques, X. Reboud, et al. (2022). A research agenda for scaling up agroecology in european countries. Agronomy for Sustainable Development 42(3), 53.

Girardin, L. (2017). Non-cooperative Fisher–KPP systems: traveling waves and long-time behavior. Nonlinearity 31(1), 108.

Griette, Q. and H. Matano (2021). Propagation dynamics of solutions to spatially periodic reaction-diffusion systems with hybrid nonlinearity. arXiv preprint arXiv:2108.10862.

Hamel, F., J. Fayard, and L. Roques (2010). Spreading speeds in slowly oscillating environments. Bulletin of Mathematical Biology 72(5), 1166–1191.

Hamel, F., G. Nadin, and L. Roques (2011). A viscosity solution method for the spreading speed formula in slowly varying media. Indiana University Mathematics Journal 60, 1229–1247.

Holzer, M. (2014). Anomalous spreading in a system of coupled Fisher–KPP equations. Physica D: Nonlinear Phenomena 270, 1–10.

Kamke, E. (2013). Differentialgleichungen Lösungsmethoden und Lösungen. Springer-Verlag.

Kawecki, T. J. and D. Ebert (2004). Conceptual issues in local adaptation. Ecology Letters 7(12), 1225–1241.

Keesing, F., R. D. Holt, and R. S. Ostfeld (2006). Effects of species diversity on disease risk. Ecology Letters 9(4), 485–498.

Keitt, T. H., M. A. Lewis, and R. D. Holt (2001). Allee effects, invasion pinning, and species' borders. The American Naturalist 157, 203–216.

Kimura, M. and T. Maruyama (1966). The mutational load with epistatic gene interactions in fitness. Genetics 54(6), 1337.

Kinezaki, N., K. Kawasaki, and N. Shigesada (2006). Spatial dynamics of invasion in sinusoidally varying environments. Population Ecology 48(4), 263–270.

Kinezaki, N., K. Kawasaki, F. Takasu, and N. Shigesada (2003). Modeling biological invasions into periodically fragmented environments. Theoretical Population Biology 64(3), 291–302.

Kirkpatrick, M. and N. H. Barton (1997). Evolution of a species'range. The American Naturalist 150, 1–23.

Lavigne, F., G. Martin, Y. Anciaux, J. Papaix, and L. Roques (2020). When sinks become sources: adaptive colonization in asexuals. Evolution 74(1), 29–42.

Lively, C. M. (2010). The Effect of Host Genetic Diversity on Disease Spread. The American Naturalist 175(6), E149–E152.

Lutscher, F., L. Popovic, and A. K. Shaw (2023). How mutation shapes the rate of population spread in the presence of a mate-finding allee effect. Theoretical Ecology 16(4), 255–269.

Maciel, G. A. and F. Lutscher (2013). How individual movement response to habitat edges affects population persistence and spatial spread. The American Naturalist 182(1), 42–52.

Maciel, G. A. and F. Lutscher (2015). Allee effects and population spread in patchy landscapes. Journal of Biological Dynamics 9(1), 109–123.

Martin, G. and S. Gandon (2010). Lethal mutagenesis and evolutionary epidemiology. Philosophical Transactions of the Royal Society B: Biological Sciences 365(1548), 1953–1963.

Mollison, D. (1991). Dependence of epidemic and population velocities on basic parameters. Mathematical Biosciences 107, 255–287.

Morris, A., L. Börger, and E. Crooks (2019). Individual variability in dispersal and invasion speed. Mathematics 7(9), 795.

Mundt, C. C. (2002). Use of multiline cultivars and cultivar mixtures for disease management. Annual Review of Phytopathology 40(1), 381–410.

Nadin, G. (2010). The effect of the Schwarz rearrangement on the periodic principal eigenvalue of a nonsymmetric operator. SIAM Journal on Mathematical Analysis 41, 2388–2406.

Okubo, A. and S. A. Levin (2002). Diffusion and Ecological Problems – Modern Perspectives. Second edition, Springer-Verlag, New York.

Papaix, J., J. J. Burdon, C. Lannou, and P. H. Thrall (2014). Evolution of Pathogen Specialisation in a Host Metapopulation: Joint Effects of Host and Pathogen Dispersal. PLOS Computational Biology 10(5), e1003633.

Papaix, J., O. David, C. Lannou, and H. Monod (2013). Dynamics of adaptation in spatially heterogeneous metapopulations. PloS One 8(2), e54697.

Papaix, J., S. Touzeau, H. Monod, and C. Lannou (2014). Can epidemic control be achieved by altering landscape connectivity in agricultural systems? Ecological Modelling 284, 35–47.

Pease, C. P., R. Lande, and J. J. Bull (1989). A model of population growth, dispersal and evolution in a changing environment. Ecology 70, 1657–1664.

Peltier, G. (2020). Accelerating invasions along an environmental gradient. Journal of Differential Equations 268(7), 3299–3331.

Poloni, S. and F. Lutscher (2023). Integrodifference models for evolutionary processes in biological invasions. Journal of Mathematical Biology 87(1), 10.

Rimbaud, L., F. Fabre, J. Papix, B. Moury, C. Lannou, L. G. Barrett, and P. H. Thrall (2021). Models of Plant Resistance Deployment. Annual Review of Phytopathology 59(1), 125–152.

Shigesada, N. and K. Kawasaki (1997). Biological Invasions: Theory and Practice. Oxford Series in Ecology and Evolution, Oxford: Oxford University Press.

Shigesada, N., K. Kawasaki, and E. Teramoto (1986). Traveling periodic-waves in heterogeneous environments. Theoretical Population Biology 30(1), 143–160.

Skellam, J. G. (1951). Random dispersal in theoretical populations. Biometrika 38, 196–218.

Skelsey, P., W. A. H. Rossing, G. J. T. Kessel, J. Powell, and W. Van Der Werf (2005). Influence of Host Diversity on Development of Epidemics: An Evaluation and Elaboration of Mixture Theory. Phytopathology 95(4), 328–338.

Wang, C.-H., S. Matin, A. B. George, and K. S. Korolev (2019). Pinned, locked, pushed, and pulled traveling waves in structured environments. Theoretical population biology 127, 102–119.

Weinberger, H. F. (2002). On spreading speeds and traveling waves for growth and migration in periodic habitat. Journal of Mathematical Biology 45, 511–548.

Weinberger, H. F., M. A. Lewis, and B. Li (2007). Anomalous spreading speeds of cooperative recursion systems. Journal of Mathematical Biology 55, 207–222.

Williams, G. C. (2018). Adaptation and natural selection: A critique of some current evolutionary thought, Volume 61. Princeton university press.

Yurk, B. P. and C. A. Cobbold (2018). Homogenization techniques for population dynamics in strongly heterogeneous landscapes. Journal of Biological Dynamics 12(1), 171–193.